

Cyclo[*m*]pyridine[*n*]pyrroles: Hybrid Macrocycles That Display Expanded π -Conjugation upon Protonation

Zhan Zhang,[†] Jong Min Lim,[‡] Masatoshi Ishida,[‡] Vladimir V. Roznyatovskiy,[†] Vincent M. Lynch,[†] Han-Yuan Gong,[†] Xiaoping Yang,[†] Dongho Kim,^{*,‡} and Jonathan L. Sessler^{*,†,‡}

[†]Department of Chemistry and Biochemistry, 1 University Station-A5300, The University of Texas at Austin, Austin, Texas 78712-0165, United States

[‡]Department of Chemistry, Yonsei University, Seoul 120-749, Korea

S Supporting Information

ABSTRACT: Novel hybrid cyclo[*m*]pyridine[*n*]pyrroles have been synthesized using Suzuki coupling. Their NMR and optical spectroscopic features and solid state structural parameters provide support for the proposal that these species are best described as locally aromatic compounds devoid of long-range intersubunit conjugation. However, an extension of the π -conjugation in the macrocycles can be realized through protonation, as inferred from optical spectroscopic and X-ray diffraction-based structural studies.

Cyclo[6]pyrroles (e.g., **1**; Figure 1) are expanded porphyrins consisting of six directly linked pyrroles.

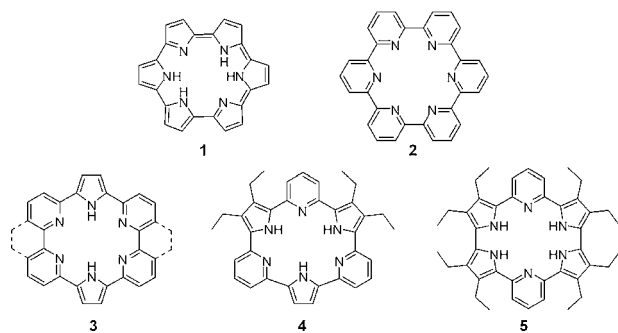


Figure 1. Representative structures of cyclo[6]pyrrole **1**, cyclo[6]pyridine **2**, and hybrid cyclo[*m*]pyridine[*n*]pyrroles **3–5**. In the case of **1–3**, the substituents have been removed for clarity.

These highly symmetric cyclophanes, typically isolated in their diprotonated forms, contain 22 π -electron peripheries and display spectroscopic and structural features characteristic of $[4n + 2]$ Hückel aromatic systems with $n = 5$.^{1,2} In the presence of the uranyl cation, cyclo[6]pyrroles undergo oxidation to produce overall neutral UO_2^{2+} complexes with Hückel antiaromatic character.³ This ability to support extended conjugation pathways stands in marked contrast to what is true for the so-called sexipyridines (cyclo[6]pyridine; e.g., **2**). These systems, first reported by Newkome⁴ and Toner⁵ in 1983 and later in a more soluble form by Bell et al.,⁶ display little evidence of electronic communication between the individual and locally aromatic 6 π -electron heterocyclic

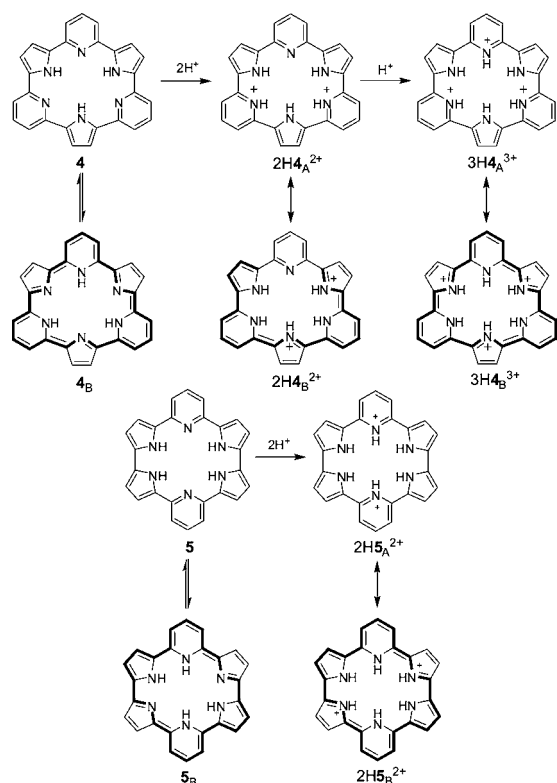
subunits. The difference in π -electron features of **1** and **2** serves to bookend what could be a continuum of analogous compounds containing a total of 6 pyridines and pyrroles. These systems, the putative cyclo[*m*]pyridine[*n*]pyrroles ($m + n = 6$), are of interest because protonation would allow for the possible stabilization of quinoid-like resonance structures and delocalization of the positive charge onto an adjacent pyrrolic heterocycle (cf. canonical forms A and B in Scheme 1).⁷ Where the number of pyrroles equals or exceeds the number of pyridines, full protonation might allow for contributions from annulene-like resonance structures wherein full electronic communication around a Hückel-type $[4n]$ or $[4n + 2]$ periphery is achieved. Previously, Müllen et al. reported the preparation of a bridged version of the cyclo[4]pyridine[2]pyrrole **3** but did not investigate its electronic structure in detail, in either its neutral or protonated forms.⁸

Here, we report the synthesis and characterization of the cyclo[3]pyridine[3]pyrrole **4** and cyclo[2]pyridine[4]pyrrole **5** and that protonation of the macrocycles results in an increase in the extent of π -electron conjugation within the macrocycles. In the case of **5**, diprotonation occurs readily. This produces a fully conjugated, annulene-like structure that reflects the presence of an electronically delocalized 24 π -electron antiaromatic resonance contributor ($2\text{H}_5\text{B}^{2+}$) within an overall structure dominated by localized aromaticity (e.g., contributor ($2\text{H}_5\text{A}^{2+}$)). Interestingly, the corresponding fully conjugated Hückel-like species (i.e., $3\text{H}_4\text{B}^{3+}$) is not an important feature of the chemistry of **4**. This is because under most conditions (both in solution and in the solid state) diprotonation, rather than triprotonation, occurs; this produces species, such as $2\text{H}_4\text{B}^{2+}$, characterized by extended π -conjugation, but which lack the full delocalization required to stabilize an $[24]$ -annulene-type antiaromatic periphery. The present results thus serve to complement more traditional approaches to controlling conjugation in porphyrinoids, which have largely relied on redox reactions and changes in the overall electron count.⁹

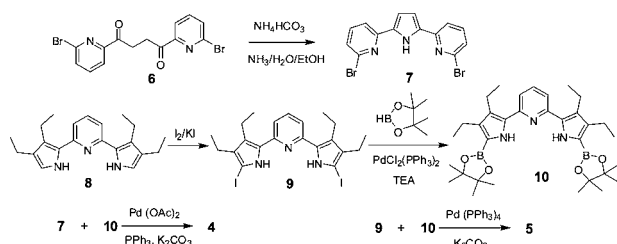
Suzuki couplings were used in the convergent synthesis of the hybrid cyclo[*m*]pyridine[*n*]pyrroles **4** and **5** (Scheme 2). The two key building blocks for the synthesis of macrocycle **4** are the linear dibromo-2,5-dipyridinylpyrrole **7** and the diboryl

Received: January 4, 2012

Published: February 14, 2012

Scheme 1. Extension of π -Conjugation Induced by Protonation of 4 and 5^a

^aSubstituents on the pyrrole rings have been removed for clarity.

Scheme 2. Synthesis of Hybrid Cyclo[*m*]pyridine[*n*]pyrroles 4 and 5

2,6-dipyrrolylpyridine **10**. Precursor **7** was prepared via the cyclization of the known bis(bromopyridine) **6**¹⁰ in excellent yield (cf. Supporting Information (SI)). The immediate precursor to **10**, the diiodide **9**, was obtained by iodination of the α -free 2,6-dipyrrolylpyridine **8**.^{8c,11} Subsequent Pd-catalyzed borylation yielded **10** in good yield. Suzuki coupling of **7** and **10** in the presence of palladium(II) acetate and triphenylphosphine in DMF–H₂O produced macrocycle **4** in 25% isolated yield when dibromide **7** was added slowly using a syringe pump. A similar Pd(PPh₃)₄ catalyzed coupling between **9** and **10** produced macrocycle **5** in 41% yield.

Crystallographic analysis of single crystals grown from tetrahydrofuran (THF)/hexanes revealed that macrocycle **4** is characterized by an essentially planar backbone in the solid state. In contrast, cyclo[2]pyridine[4]pyrrole **5** displays a slightly ruffled structure in the solid state, wherein the pyrrole rings are tilted off an otherwise planar core (Figure 2). The pyridine and pyrrole nitrogen atoms define a near-ideal hexagonal cavity in the case of **4** but a slightly pinched one

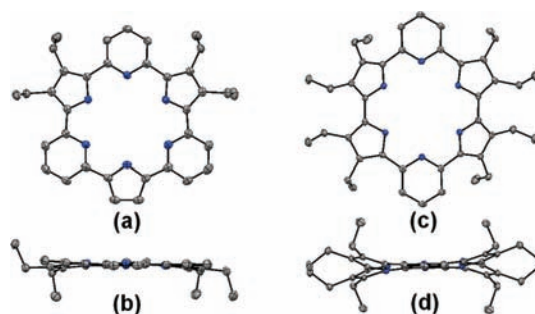


Figure 2. Single crystal X-ray structures of neutral macrocycles **4** and **5**: (a) Top and (b) side view of **4**; (c) top and (d) side view of **5**. The thermal ellipsoids are scaled to the 50% probability level. H-atoms have been removed for clarity.

in the case of **5**. Both macrocycles have cavities that are slightly larger than reported for the structurally characterized cyclo[6]-pyrroles.^{1,3} For instance, the average distance of the diagonal Ns is 5.43 Å for **4** and 5.42 Å for **5**. On the other hand, this parameter is 5.29 Å for cyclo[6]pyrrole in its free-base form.¹ Both the pyrrole and pyridine rings in macrocycles **4** and **5** are characterized by bond lengths and angles that are typical for locally aromatic heterocycles.

Proton NMR spectroscopic analysis revealed that the hybrid cyclo[*m*]pyridine[*n*]pyrroles **4** and **5** in their neutral forms are nonaromatic as inferred from the recorded chemical shift values. For instance, the inner NH proton signals were observed in the range of 9–11 ppm. This corresponds to the chemical shifts typical of pyrrole NH protons in nonaromatic compounds.¹² Likewise, the peripheral pyridine protons were found to resonate between 7 and 8 ppm. Such shifts are in line with what is expected for this subunit when not included in an aromatic or antiaromatic periphery (cf. SI).¹³ These chemical shift values thus provide further support for the conclusion that the hybrid macrocycles **4** and **5** are more sexipyridine-like than cyclo[6]pyrrole-like in terms of their electronic character. In other words, contributions from Hückel-type 24 π -electron forms, such as **4_B** and **5_B**, are minimal (Scheme 1). This is not surprising since the structures in question are unstable zwitterionic quinoid-type species.

As expected for compounds devoid of extended conjugation, neither **4** nor **5** displayed a long-range absorption band over 500 nm in their respective UV–vis spectra as recorded in either toluene or dichloromethane (Figure 3 and SI). Both cyclo[*m*]-

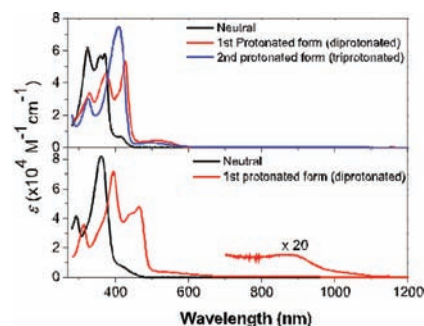


Figure 3. Steady-state absorption spectra of (top) neutral **4** (black) and its protonated forms (red, diprotonated; blue, triprotonated) and (bottom) neutral **5** and its diprotonated form (red) obtained upon addition of methanesulfonic acid (MSA) in CH₂Cl₂.

pyridine[*n*]pyrrole species **4** and **5** exhibit fluorescence emission bands in the region of 450–700 nm. Moreover, their fluorescence lifetimes are estimated as 5.4 and 4.9 ns, respectively (SI).

Significant changes in the spectral features of **4** and **5** were observed upon protonation. The major UV–vis absorption bands of **4** and **5** underwent a 50–100 nm red shift upon treatment with trifluoroacetic acid (TFA) in dichloromethane. Interestingly, treatment with ca. 2.5 equiv of TFA served to quench the fluorescence of **5** but shifted the emission of **4** to longer wavelengths. Specifically, a fluorescence emission band at $\lambda_{\text{max}} = 597$ nm was seen for **4** in dichloromethane upon the addition of TFA (cf. SI). This is tentatively ascribed to the fact that full protonation of **4** is not achieved under these conditions and that contributions from antiaromatic resonance contributors, such as $3\text{H}4_{\text{B}}^{3+}$, are thus unimportant in contrast to what is true for **5**, where full conjugation can be achieved as reflected in structure $2\text{H}5_{\text{B}}^{2+}$. Consistent with this observation, diprotonation of **4** and **5** in the solid state occurs readily, as revealed by X-ray diffraction analysis of single crystals generated in the presence of an excess of TFA (cf. SI).

The diprotonated product $2\text{H}4^{2+}$ formed using TFA was further characterized in the solid state by recording the fluorescence spectrum within a KBr pellet (Figure 4). KBr

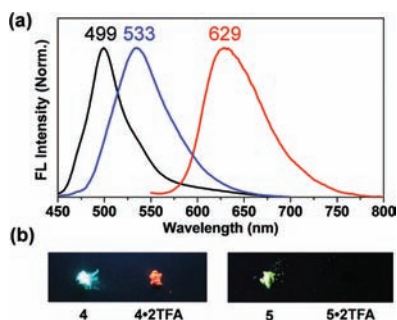


Figure 4. (a) Fluorescence emission spectra of **4** (black line), **5** (blue), and **4•2TFA** (red) recorded for KBr pellets ($\lambda_{\text{ex}} = 370$ nm for **4** and **4•2TFA**; 360 nm for **5**). (b) Photographs of powder samples of **4**, **5**, **4•2TFA**, and **5•2TFA** as seen under a UV-lamp (365 nm).

pellets of salt **4•2TFA** exhibit a red emission centered at 629 nm, which is in good agreement with the corresponding spectral features obtained in solution with TFA (vide supra).

In an effort to obtain the triprotonated form of **4**, analogous titrations were carried out with a stronger acid, methanesulfonic acid (MSA) (Figure 3). These titrations gave rise to qualitatively similar changes in the absorption spectrum at least initially. For instance, test studies carried out with **5** and 2 equiv of MSA produced the same species as was seen in the presence of excess TFA (≥ 3 equiv). On the other hand, the addition of excess MSA to **4** in dichloromethane led to the production of a UV–vis absorption spectrum that was different from both the free base and that produced with excess TFA. Upon protonation with excess MSA, the small, relatively low-energy absorption band centered around 510 nm was seen to decrease. Meanwhile the major absorption band at 432 nm shifts to the blue and appears at 409 nm. Although such further spectral changes were not seen in the case of **5**, the diprotonated form of **5** produced with MSA shows a weak but significant NIR absorption band around 900 nm (Figure 3). Interestingly, this NIR band is solvent-dependent and was not

observed when the analogous titration was carried out in toluene.

Based on the number of equivalents needed to produce the first set of changes and the corresponding solid state structural analyses, it is suggested that the species obtained in the presence of excess TFA and small quantities of MSA are the diprotonated forms of **4** and **5**, respectively. In the specific case of **4** studied in dichloromethane, conversion of this diprotonated form to the corresponding triprotonated form occurs at least to some extent in the presence of excess MSA in CH_2Cl_2 , but not in the presence of TFA in toluene. We thus believe that full protonation of **4** is only achievable under forcing conditions and that the fully protonated form, including conjugated 24 π -electron resonance structures (e.g., $3\text{H}4_{\text{B}}^{3+}$), does not play an important role in the chemistry of **4** under most solution phase conditions. Presumably, this reflects the fact that full protonation would put three positive charges within the center of the ring. Steric considerations, namely the absence of sufficient space within the macrocyclic core to accommodate a third acid without distortion, could also play a role in reducing the effective basicity of the system, as is true for porphyrins.¹⁴

The red shifts in the absorption bands seen for both **4** and **5** in the presence of TFA or MSA are attributed to an extension of the π -conjugation pathway brought about by protonation. As shown in Scheme 1, protonation results in the placement of positive charge on the basic pyridine N-atoms. These charges can be delocalized onto the neighboring pyrrole N-atoms through resonance and associated extension of the π -conjugation pathway.

Support for this supposition came from spectroscopic studies of **4** and **5** and their protonated forms, specifically analyses of their fluorescence lifetimes and excited-state dynamics (SI). In accord with what would be expected given the near complete loss of fluorescence emission intensity, the diprotonated form of **5** with MSA in dichloromethane showed very fast excited-state decay dynamics with time components of 0.9 and 32 ps. However, in the case of **4**, the diprotonated form produced with 2.5 equiv of MSA in toluene showed a single exponential decay profile with a lifetime of 1.3 ns, a value that is in good agreement with its fluorescence lifetime of 1.2 ns. Upon treatment with excess MSA, the fluorescence of **4** is mostly quenched. On the basis of the structure–property relationship between molecular conformation, photophysical properties, and aromaticity established for polypyrrolic macrocyclic systems,¹⁵ we ascribe the changes in the spectroscopic features seen for **4** and **5** upon protonation to the formation of species with an extended π -conjugation and, in the specific case where the triprotonated form of **4** is formed, the accompanying buildup of antiaromatic character.

To obtain further insight into the electronic features of cyclo[*m*]pyridine[*n*]pyrroles in their neutral and protonated forms, we performed TD-DFT calculations using the Gaussian09 package. The simulated absorption spectra of macrocycles **4** and **5** were found to match well with the experimental data (SI). Upon protonation, the energy gaps between the HOMO and LUMO in **4** and **5** are reduced as compared to those of the neutral forms. The lowest absorption bands in the protonated forms are seen to originate from the transition between the HOMO and LUMO orbitals. Interestingly, the LUMO+1 and LUMO+2 orbitals are calculated to be degenerate in the case of both $3\text{H}4^{3+}$ and $2\text{H}5^{2+}$ (cf. SI). In analogy to what is true for antiaromatic expanded porphyr-

inoids, this feature results in configuration interactions among each of the orbitals in question.¹⁵ Finally, as inferred from its calculated electronic structure, which is more complex than that of 2H_5^{2+} (cf. SI), the fully antiaromatic triprotonated form of **4** (3H_4^{3+}) is expected to display a relatively short excited state lifetime and be weakly fluorescent, as seen by experiment (vide supra).

Further support for the proposed protonation-induced π -extension in **4** and **5** came from the investigation of the structural parameters for their neutral and protonated forms (SI). In the case of the neutral forms of **4** and **5** the average pyrrole–pyrrole and pyrrole–pyridine bond lengths (1.464 ± 0.005 and 1.458 ± 0.003 , respectively) are close to those expected for a typical $\text{C}(\text{sp}^2)\text{--C}(\text{sp}^2)$ single bond and hence noticeably longer than what is seen in the case of cyclo[6]-pyrrole (1.428 ± 0.002 Å).^{1,3} In the diprotonated species 2H_5^{2+} , the average length of these bonds is shortened to 1.449 ± 0.006 , 1.448 ± 0.01 , and 1.443 ± 0.01 Å in the case of the TFA, MSA, and HCl salts, respectively. In the case of the diprotonated species **4**•2TFA, the average C–C bond length between the protonated pyridine and pyrrole subunits is shortened (1.443 ± 0.008 Å) as compared to what is seen for the bonds flanking the neutral pyridine in this salt ($C_{\text{pyrrole}}\text{--}C_{\text{pyridine}}$ distance = 1.459 ± 0.01 Å). Protonation also produces changes in the C–N–C bond angles on the protonated pyridine rings. In the neutral forms of **4** and **5** an average bond angle of 119° was observed. In contrast, an average bond angle of 124° was seen in the protonated species **4**•2TFA and **5**•2TFA. A relatively large C–N–C angle of 125.8° has also been seen in a protonated 2-pyridylimido derivative, which could reflect contributions from cationic pyridinium and pyridinylidene resonance structures.¹⁶ These observations are consistent with the buildup of greater interheterocycle double bond character upon protonation of **4** and **5**.

To examine further the effect of the putative extended conjugation and its possible effect on the global electronic features of **4** and **5**, the HOMA (Harmonic Oscillator Model of Aromaticity) indices of both the neutral forms and their protonated forms were calculated. The average values of 0.716 and 0.738 for **4** and **5**, respectively, were seen to increase to 0.790, 0.791, 0.788, and 0.810 for **4**•2TFA, **5**•2TFA, **5**•2MSA, and **5**•2HCl, respectively. (cf. SI).

In summary, two types of novel hybrid cyclo[*m*]pyridine-[*n*]pyrroles **4** and **5** have been synthesized using a Suzuki cross-coupling strategy. These neutral forms of **4** and **5** are best considered to be nonaromatic macrocycles. Protonation of **4** and **5** leads to an extension of the π -conjugation as supported by spectroscopic and crystallographic studies as well as DFT calculations. In particular, a 24π -electron Hückel antiaromatic contributor (2H_5^{2+}) is thought to account for the observed feature of the diprotonated form of this bis-pyridine cyclo[6]-pyrrole analogue, as reflected, e.g., in the observed NIR absorption band and short excited state lifetime. In the case of **4**, the addition of acid results in the formation of a diprotonated species under most conditions. However, under forcing conditions a triprotonated species, for which a degree of antiaromatic character is inferred, is obtained.

■ ASSOCIATED CONTENT

Supporting Information

Synthetic experimental, additional spectroscopic information, and structural data. This material is available free of charge via the Internet at <http://pubs.acs.org>.

■ AUTHOR INFORMATION

Corresponding Author

dongho@yonsei.ac.kr; sessler@mail.utexas.edu

Notes

The authors declare no competing financial interest.

■ ACKNOWLEDGMENTS

Support is acknowledged from the U.S. National Science Foundation (Grant CHE-1057904 to J.L.S.), the WCU (World Class University) program (R32-2010-000-10217-0) of the National Research Foundation of Korea funded by the Ministry of Education, Science and Technology, and the Cancer Research and Prevention Institute of Texas for a postdoctoral traineeship to Z.Z.

■ REFERENCES

- (1) Köhler, T.; Seidel, D.; Lynch, V.; Arp, F. O.; Ou, Z.; Kadish, K. M.; Sessler, J. L. *J. Am. Chem. Soc.* **2003**, *125*, 6872–6873.
- (2) Yoon, Z. S.; Kwon, J. H.; Yoon, M.-C.; Koh, M. K.; Noh, S. B.; Sessler, J. L.; Lee, J. T.; Seidel, D.; Aguilar, A.; Shimizu, S.; Suzuki, M.; Osuka, A.; Kim, D. *J. Am. Chem. Soc.* **2006**, *128*, 14128–14134.
- (3) Melfi, P. J.; Kim, S. K.; Lee, J. T.; Bolze, F.; Seidel, D.; Lynch, V. M.; Veauthier, J. M.; Gaunt, A. J.; Neu, M. P.; Ou, Z.; Kadish, K. M.; Fukuzumi, S.; Ohkubo, K.; Sessler, J. L. *Inorg. Chem.* **2007**, *46*, 5143–5145.
- (4) Newkome, G. R.; Lee, H.-W. *J. Am. Chem. Soc.* **1983**, *105*, 5956–5957.
- (5) Toner, J. L. *Tetrahedron Lett.* **1983**, *24*, 2707–2710.
- (6) Bell, T. W.; Firestone, A. *J. Am. Chem. Soc.* **1986**, *108*, 8109–8111.
- (7) Such delocalization effects have previously been suggested in the case of pyridyl porphyrin analogues, albeit not studied in detail; cf. (a) Mysliborski, R.; Latos-Grazynski, L.; Szyterenberg, L. *Eur. J. Org. Chem.* **2006**, 3064–3068. (b) Lash, T. D.; Pokharel, K.; Serling, J. M.; Yant, V. R.; Ference, G. M. *Org. Lett.* **2007**, *9*, 2863–2866.
- (8) (e) Norouzi-Arasi, H.; Pisula, W.; Mavrinskiy, A.; Feng, X.; Müllen, K. *Chem.—Asian J.* **2011**, *6*, 367–371. For examples of macrocycles containing pyridine and pyrrole, see: (a) Arnold, L.; Norouzi-Arasi, H.; Wagner, M.; Enkelmann, V.; Müllen, K. *Chem. Commun.* **2011**, 970–972. (b) Setsune, J.-i.; Kawama, M.; Nishinaka, T. *Tetrahedron Lett.* **2011**, *52*, 1773–1777. (c) Setsune, J.-i.; Watanabe, K. *J. Am. Chem. Soc.* **2008**, *130*, 2404–2405. (d) Král, V.; Gale, P. A.; Anzenbacher, P. Jr.; Jursiková, K.; Lynch, V.; Sessler, J. L. *Chem. Commun.* **1998**, 9–10.
- (9) (a) Muranaka, A.; Ohira, S.; Hashizume, D.; Koshino, H.; Kyotani, F.; Hirayama, M.; Uchiyama, M. *J. Am. Chem. Soc.* **2012**, *134*, 190–193. (b) Mori, S.; Kim, K. S.; Yoon, Z. S.; Noh, S. B.; Kim, D.; Osuka, A. *J. Am. Chem. Soc.* **2007**, *129*, 11344–11345. For reviews, see: (c) Osuka, A.; Saito, S. *Chem. Commun.* **2011**, 4330–4339. (d) Sessler, J. L.; Seidel, D. *Angew. Chem., Int. Ed.* **2003**, *42*, 5134–5175.
- (10) Owsley, D. C.; Nelke, J. M.; Bloomfield, J. J. *J. Org. Chem.* **1973**, *38*, 901–903.
- (11) Setsune, J.-i.; Toda, M.; Watanabe, K.; Panda, P. K.; Yoshida, T. *Tetrahedron Lett.* **2006**, *47*, 7541–7544.
- (12) The NH protons of precursors **7** and **9** resonate in this range.
- (13) In unsubstituted sexipyridine the corresponding resonance is found at 7.8–8.1 ppm. Cf. ref 4.
- (14) Stone, A.; Fleischer, E. B. *J. Am. Chem. Soc.* **1968**, *90*, 2735–2748.
- (15) Cho, S.; Yoon, Z. S.; Kim, K. S.; Yoon, M.-C.; Cho, D.-G.; Sessler, J. L.; Kim, D. *J. Phys. Chem. Lett.* **2010**, *1*, 895–900.
- (16) Amanov, R. U.; Matrosov, E. L.; Antipin, M. Y.; Khodak, A. A.; Matveeva, E. L.; Policarpov, Y. M.; Sharipov, K. T.; Struchkov, Y. T.; Kabachnik, M. L. *Russian Chem. Bull.* **1993**, *42*, 77–81.